Journal of ELECTRONIC MATERIALS, Vol. 44, No. 8, 2015
DOI: 10.1007/s11664-015-3757-x
© 2015 The Minerals, Metals & Materials Society

SiC Nitridation by NH_3 Annealing and Its Effects in MOS Capacitors with Deposited SiO_2 Films

E. PITTHAN,[1,5] A.L. GOBBI,[2] H.I. BOUDINOV,[1,3] and F.C. STEDILE[1,4]

1.—PGMICRO, UFRGS, Porto Alegre, RS 91509-900, Brazil. 2.—Laboratório Nacional de Nanotecnologia, Campinas, SP 13083-100, Brazil. 3.—Instituto de Física, UFRGS, Porto Alegre, RS 91509-900, Brazil. 4.—Instituto de Química, UFRGS, Porto Alegre, RS 91509-900, Brazil. 5.—e-mail: eduardo.pitthan@ufrgs.br

Silicon carbide (SiC) thermal nitridation followed by oxide deposition is a route to confine nitrogen at the SiO_2/SiC interfacial region. To investigate its effects, incorporation of nitrogen into SiC by annealing in isotopically enriched ammonia was performed. This incorporation led mainly to silicon nitride-like formation. The observed silicon oxynitrides originated mainly from oxygen incorporation due to air exposure of samples. Metal–oxide–semiconductor structures formed by SiO_2 deposition on nitrided SiC samples presented poor electrical quality, even when different postdeposition annealing conditions in argon were applied. Such results suggest that this route must be modified to allow nitrogen incorporation and avoid electrical degradation.

Key words: SiO_2/SiC interface, ammonia annealing, nuclear reaction analyses, isotopes, MOS capacitors, sputtered SiO_2 films

The properties of silicon carbide (SiC) make it a suitable semiconductor to replace Si in devices required for high-power, high-frequency, and/or high-temperature applications. Besides, a dielectric film of silicon dioxide (SiO_2) can be thermally grown on it, in a similar way as on Si,[1,2] but the density of SiO_2/SiC interface states (D_{it}) of thermally grown films is orders of magnitude higher than for SiO_2/Si, limiting the electrical quality of SiC-based metal–oxide–semiconductor field-effect transistors (MOSFETs).[3]

Postoxidation annealing (POA) in nitric oxide (NO) is a well-known method to efficiently reduce the SiO_2/SiC D_{it} and increase channel mobilities of SiC MOSFETs.[3,4] This method provides passivation of defects by incorporating sub-monolayer amounts of nitrogen in the interfacial region,[5,6] as well as reducing the SiO_2/SiC transition-layer thickness.[7,8] A "counterdoping" effect[9,10] due to nitrogen has also been proposed as a main cause of the increased channel mobility: nitrogen incorporated in SiC would act as an n-type donor in a thin layer of the SiC wafer. However, since two molecules of NO can thermally dissociate into N_2 and O_2,[11,12] one limitation of this method is the competition between nitrogen passivation and the SiC electrical degradation induced by thermal oxidation.[13] Thus, there is great interest in investigation of alternative routes to introduce nitrogen into the SiO_2/SiC interfacial region, aiming at reducing D_{it} but without inducing electrical degradation due to oxygen incorporation. One simple solution to achieve this goal would be to substitute NO by a non-oxygen-containing gas such as ammonia (NH_3) or molecular nitrogen (N_2). Due to the higher thermal stability of N_2, nitrogen passivation by POA is achieved using a nitrogen plasma.[14–16] However, defects can be introduced in the oxide due to the plasma exposure, resulting in low oxide breakdown strength compared with samples submitted to NO POA. Use of NH_3 could be beneficial, since a nitrogen/hydrogen synergistic effect in SiO_2/SiC D_{it} reduction has already been reported.[17] In fact, SiO_2/SiC POA in NH_3 can also reduce D_{it} in a similar way to NO annealing.[18,19] The difference is that, while in NO POA nitrogen is incorporated only into the SiO_2/SiC interfacial region, in the case of ammonia, nitrogen

(Received February 3, 2015; accepted March 19, 2015; published online April 11, 2015)

is incorporated into the SiO_2 film surface, bulk, and interface, reducing the oxide film dielectric strength.[3,19]

Direct nitridation of the SiC substrate followed by oxide deposition is another approach used to form MOS structures, confining nitrogen to the SiO_2/SiC interfacial region. Such incorporation of N has been achieved by annealing SiC in H_2 followed by N_2,[20] by annealing SiC in a mixture of N_2 and NH_3,[21] and by nitrogen plasma irradiation[22] of the SiC surface prior to oxide deposition, resulting in a reduction of D_{it} compared with thermally grown oxide films. Nevertheless, several aspects concerning SiC nitridation followed by oxide film deposition still need to be investigated, such as how the nitrogen source and nitridation conditions affect the SiO_2/SiC interface quality, whether the breakdown strength of the deposited oxide film is sufficient for use in a MOSFET, and whether postdeposition annealing (PDA) is necessary to improve the structural quality. Overall, is such a route advantageous compared with standard NO annealing? To investigate such points, better comprehension of the interaction of nitrogen-containing gas with SiC and its consequences for the resulting MOS structure must be achieved.

In this work, nitrogen incorporation in clean 4H-SiC samples by thermal nitridation in ammonia gas was investigated. Isotopically enriched ammonia ($^{15}NH_3$) was used to allow quantification and depth profiling of ^{15}N by nuclear reaction analysis (NRA). Ammonia was used in this work due to its higher reactivity compared with other nitrogen-containing gases that are oxygen-free, and due to its hydrogen content, which could be beneficial for passivation of SiO_2/SiC D_{it}. Besides nuclear reaction analysis, x-ray photoelectron spectroscopy (XPS) was used to investigate the chemical environment of atoms in these samples. Oxide deposition was performed by sputtering, and electrodes were added to produce MOS capacitors with nitrogen confined to the SiO_2/SiC interface. To correlate the results obtained by NRA and XPS with the electrical properties, current–voltage (*I*–*V*) measurements were also performed. PDA in argon under different conditions was then performed, aiming to obtain electrical improvements in the MOS structure. Ar-annealed samples were also characterized by *I*–*V* measurements and nuclear reaction analysis.

Commercial SiC wafers of 4H polytype, polished on the Si-face, also named (0001), and Si (100) wafers were employed as substrates. Samples characterized by electrical measurements were 4H-SiC (*n*-type) commercial epitaxial wafers, 8° off-axis on the Si face, doped with nitrogen (1.1×10^{16} cm^{-3}), 4.6 μm thick. SiC wafers were purchased from CREE Inc. All substrates were cleaned in a mixture of H_2SO_4 and H_2O_2 followed by the standard Radio Corporation of America (RCA) process.[23] Then, samples were etched for 60 s in 1 vol.% aqueous solution of hydrofluoric acid (40 wt.% HF, purchased from Merck) and rinsed in deionized water. Immediately after blow-drying with N_2, 4H-SiC samples were loaded into a static pressure, quartz tube, resistively heated furnace that was pumped down to 10^{-7} mbar. Nitridations of clean 4H-SiC were performed for 1 h at different temperatures with 30 mbar of NH_3 enriched to 98% in the ^{15}N isotope, denoted $^{15}NH_3$. In some of the experiments, dry O_2 (< 1 ppm H_2O) enriched to 97% in the ^{18}O isotope, denoted $^{18}O_2$, was also used. The total amount of ^{15}N and ^{18}O in the resulting samples was determined by nuclear reaction analysis (NRA) using the nuclear reactions $^{15}N(p,\gamma)^{12}C$ at 1 MeV and $^{18}O(p,\alpha)^{15}N$ at 730 keV,[24] respectively, referenced to a standard $Si_3^{15}N_4$ film on Si and to a standard $Si^{18}O_2$ film on Si.[25] ^{15}N profiles were determined using the narrow resonance of the $^{15}N(p,\alpha\gamma)^{12}C$ nuclear reaction at 429 keV. ^{15}N profiles were determined from experimental excitation curves (particle yield versus incident proton energy) using the FLATUS code.[26] SiO_2 films were deposited by radio frequency (RF) sputtering using a SiO_2 target. The deposition system was pumped down to 10^{-8} mbar, then Ar was introduced into the chamber at constant flux, keeping the pressure at 2.7×10^{-3} mbar during sputtering. PDA was performed under 400 mbar of Ar for 1 h at different temperatures in the same static pressure reactor used for nitridations. Such PDAs in Ar were performed in an attempt to improve electrical properties, as has been reported for SiO_2/SiC samples.[27] XPS analyses were performed in an Omicron-SPHERA station, using Al K_α radiation at 14° take-off angle (sensitive to the sample surface). Aluminum thermal evaporation to obtain MOS structures used a mechanical mask, forming circular capacitors with diameter of 200 μm. InGa eutectic was used as back contact. *I*–*V* curves of samples were obtained using a computer-controlled HP4155A semiconductor parameter analyzer.

The total amounts of ^{15}N obtained by NRA in Si and 4H-SiC substrates after annealing in $^{15}NH_3$ at different temperatures are presented in Table I, as well as the estimated film thickness, assuming stoichiometric Si_3N_4 film. The higher resistance to nitrogen incorporation of SiC compared with the Si substrate is clear, with one order of magnitude higher amounts of nitrogen in the Si case. It is interesting to remember that oxygen incorporation from thermal oxidation of both substrates also yields around order of magnitude higher amounts of oxygen in the Si case. Larger areal densities of nitrogen can also be observed when the temperature is increased for both substrates.

In XPS spectra of the Si 2*p* region of nitrided 4H-SiC presented in Fig. 1, three distinct components can be observed in all samples: silicon bonded to carbon (substrate), silicon bonded to nitrogen, and a component that was assigned to silicon bonded to oxygen and nitrogen and/or silicon bonded only to oxygen, since line widths and spectrometer

Table I. ^{15}N areal density and film thickness in 4H-SiC (Si face) and Si samples after thermal nitridation in 30 mbar of $^{15}NH_3$ for 1 h at different temperatures

	4H-SiC		Si	
$^{15}NH_3$ Annealing Temperature (°C)	^{15}N Amount (10^{15} $^{15}N/cm^2$)	Thickness (nm)[a]	^{15}N Amount (10^{15} $^{15}N/cm^2$)	Thickness (nm)[a]
900	0.3	0.05	3.0	0.56
1000	1.1	0.20	4.2	0.79
1100	1.8	0.34	12.4	2.33

Experimental accuracy 10%; [a]Assuming stoichiometric Si_3N_4 film.

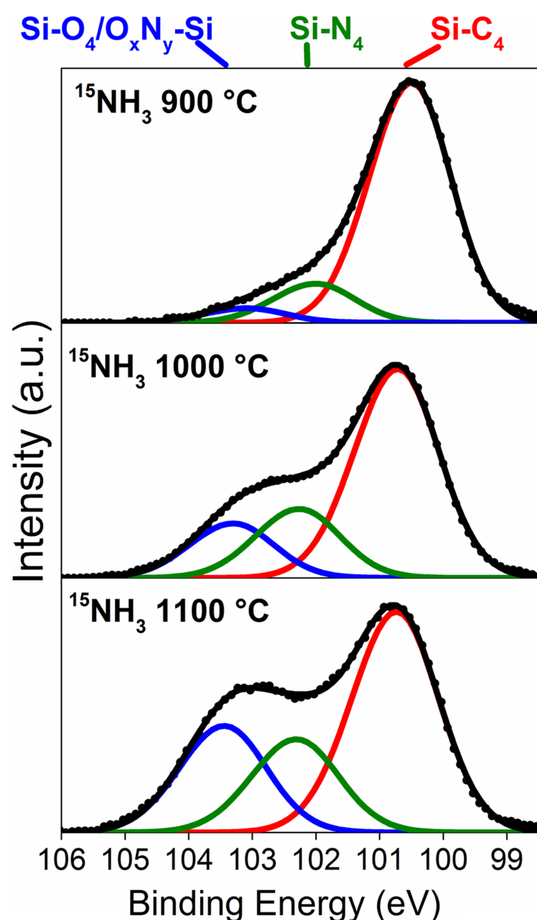

Fig. 1. Si 2*p* photoelectron spectra (a.u. stands for arbitrary units) at a take-off angle sensitive to the surface of Si-faced 4H-SiC samples thermally nitrided in 30 mbar of $^{15}NH_3$ for 1 h at different temperatures, as indicated.

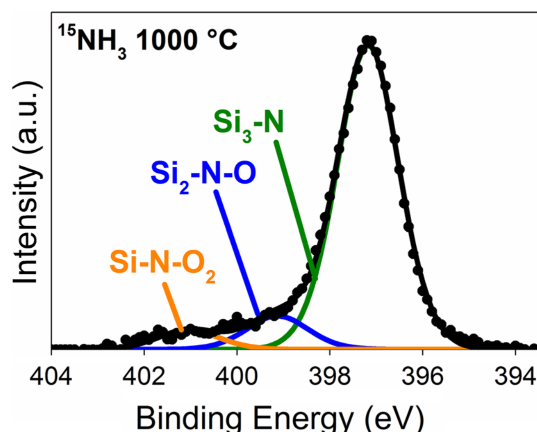

Fig. 2. N 1*s* photoelectron spectrum (a.u. stands for arbitrary units) at a take-off angle sensitive to the surface of the Si-faced 4H-SiC sample thermally nitrided in 30 mbar of $^{15}NH_3$ for 1 h at 1000°C.

resolution prevent distinction between these two latter components. The increase of the intensity of the components of silicon bonded to nitrogen with temperature as compared with the substrate signal is clear, in qualitative agreement with the NRA results. Three components can also be observed in XPS analysis in the N 1*s* region for the nitrided 4H-SiC in Fig. 2. Because for all investigated temperatures a similar signal was observed (although presenting different intensities, due to different nitrogen incorporation amounts), only the spectrum of the 1000°C nitrided sample is shown. It is interesting to note that the signal obtained from N 1*s* is similar in energy and component intensities to those obtained from SiO_2/SiC annealed in NO followed by chemical removal of the oxide,[6] suggesting a similar chemical environment for nitrogen. The most intense component is the one assigned to nitrogen bonded only to silicon, suggesting that nitrogen incorporates mainly in a silicon nitride-like form. The other components are assigned to nitrogen bonded to oxygen and to silicon in different stoichiometries. Some discrepancy concerning the proportion between silicon oxynitride and silicon nitride signals from the Si 2*p* and N 1*s* regions of the XPS spectra can be assigned to part of the silicon oxynitride signal in the Si 2*p* region being from silicon bonded only to oxygen, as in SiO_2, which is not probed in the N 1*s* spectra.

Although the presence of oxygen observed in XPS spectra is undesirable, oxygen has been observed after SiC nitridation even when working with oxygen-free gases.[20,21,28] The origin of oxygen could be due to contamination in the furnace used for

thermal nitridation or to oxygen incorporation from air exposure. Contamination in the furnace was minimized by pumping the system down to 10^{-7} mbar prior to the introduction of $^{15}NH_3$ gas, although the presence of oxygen during annealing cannot be ruled out, since the same furnace was previously used for thermal oxidations, and outdiffusion of O from its walls could occur during ammonia annealing. Incorporation from air exposure is also reasonable, since oxygen incorporation into Si_3N_4 film surfaces from air exposure after thermal nitridation of Si has been observed.[24] To investigate this second possibility in our samples, the following experiment was performed: After thermal nitridation of 4H-SiC in $^{15}NH_3$, the sample, kept in the furnace tube, was pumped down to 10^{-7} mbar and then exposed to 100 mbar of enriched $^{18}O_2$ at ambient temperature for 4 h prior to its exposure to air. If oxygen could be incorporated from air exposure, larger amounts of ^{18}O would be observed in samples exposed to $^{18}O_2$ (used to simulate air exposure in this experiment). The total amount of ^{18}O quantified by NRA of these samples can be observed in Fig. 3, compared with samples exposed directly to air after nitridation. Although all ^{18}O areal densities are considerably small, it is clear that larger amounts of ^{18}O were incorporated in samples exposed to $^{18}O_2$ compared with those exposed directly to air (in which the ^{18}O abundance is 0.2%). This confirms that a significant part of the oxygen detected in the samples by XPS measurements, which were performed *ex situ*, can be assigned to their exposure to air.

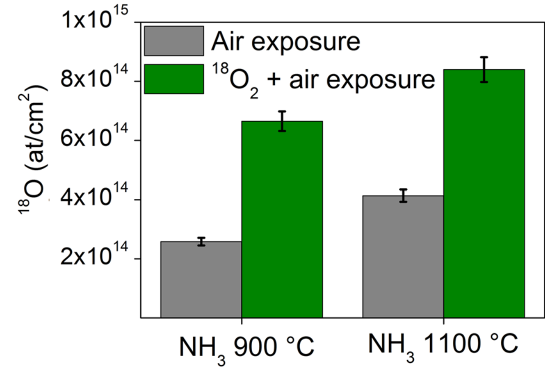

Fig. 3. ^{18}O areal densities obtained by ^{18}O NRA from 4H-SiC samples submitted to 30 mbar of $^{15}NH_3$ for 1 h at 900°C and 1100°C, followed by air exposure or exposure to 100 mbar of $^{18}O_2$ for 4 h at ambient temperature (24°C) and then exposed to air. Bars correspond to experimental accuracy of 5%.

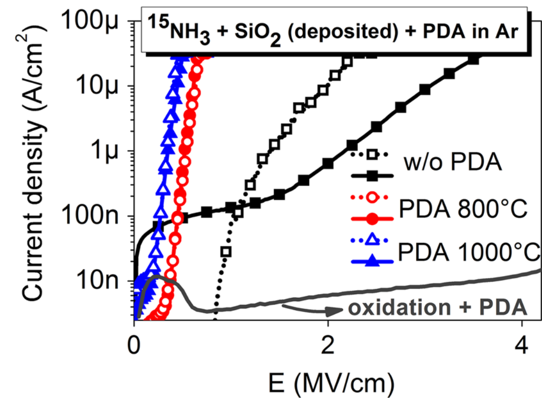

Fig. 4. *I–V* curves of Al/SiO_2/(nitrided)4H-SiC structures obtained from 4H-SiC samples submitted to 30 mbar of $^{15}NH_3$ for 1 h at 900°C (solid symbols) and 1100°C (open symbols) followed by deposition of a 20-nm oxide film by sputtering and addition of Al and GaN contacts. Indicated samples were submitted to PDA in 400 mbar of Ar for 1 h at indicated temperatures. Results from a SiO_2 film formed by SiC thermal oxidation submitted to PDA at 1000°C are also presented for comparison.

I–V curves allow one to probe the quality of dielectric films, but no previous reports were found in the case of SiO_2 films deposited on nitrided SiC. To investigate the electrical quality of the formed structures and their applicability in SiC devices, *I–V* curves from Al/SiO_2/(nitrided)4H-SiC capacitors were obtained from 4H-SiC samples nitrided in $^{15}NH_3$ at the two extreme temperatures: 900°C and 1100°C followed by SiO_2 film deposition (20 nm) by sputtering. *I–V* curves of these samples are presented in Fig. 4, as well as curves from similar samples followed by PDAs in Ar at 800°C or 1000°C and from a SiO_2 film formed by SiC thermal oxidation followed by PDA in Ar at 1000°C, included for comparison. Poor dielectric strength in the structures can be observed for all nitrided/deposited samples as a fast increase in leakage current in the initial stages of accumulation. Such results complement data from our recent work indicating low leakage current and negative effective charge of SiO_2 films thermally grown on SiC and oxide films deposited by sputtering on SiC.[29] Comparing results from samples without PDA, the larger increase of leakage current with voltage observed in the sample nitrided at a higher temperature (that led to higher incorporation of nitrogen) suggests poorer electrical quality between the nitrided SiC surface and the deposited oxide. This result indicates that a modification to this route must be accomplished to enhance the oxide strength. A possibility could be to nitride a thin SiO_2 film prior to the oxide film deposition. After the PDAs in Ar, an even larger increase in leakage current with voltage is observed, where higher PDA temperature induced larger leakage current, independent of the $^{15}NH_3$ annealing temperature.

The increase in the leakage current with voltage due to PDA in Ar was not expected, since, in general, improvement in SiO_2/SiC structures due to PDA and POA in Ar has been reported.[27,30,31] On the other hand, some reports suggest degradation of SiO_2/SiC structures due to annealing in Ar.[32,33] Since it is reported that presence of nitrogen in the bulk of the oxide film can reduce its dielectric strength,[3,19] atomic transport of ^{15}N due to PDA in Ar was also investigated. Figure 5 presents the excitation curves obtained by ^{15}N nuclear reaction

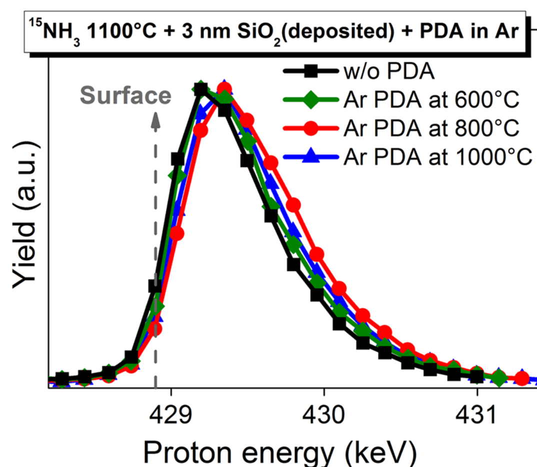

Fig. 5. Experimental excitation curves of the $^{15}N(p,\alpha\gamma)^{12}C$ nuclear reaction around the resonance at 429 keV for 4H-SiC samples nitrided for 1 h in 30 mbar of $^{15}NH_3$ at 1100°C followed by sputtering deposition of a 3-nm SiO_2 film and submitted or not to PDA in 400 mbar of Ar for 1 h at different temperatures, as indicated. A $Si_3^{15}N_4$ film was also analyzed to obtain the "surface" position indicated in the figure.

profiling (NRP) for 4H-SiC samples nitrided in $^{15}NH_3$ followed by 3-nm oxide film deposition by sputtering without and with PDA in Ar at different temperatures. Thinner oxide films were deposited compared with those used in electrical measurements to avoid NRP depth resolution degradation, but still allowing investigation of the SiO_2(deposited)/(nitrided)4H-SiC structure. The intention was to observe whether nitrogen would diffuse into the deposited oxide film due to the thermal treatment in argon. If so, a shift in the excitation curve to lower proton energies (in the direction of "surface" in the figure) due to the PDA in Ar would be observed, as was the case of oxygen from $Si^{18}O_2$ films thermally grown on SiC in the SiO_2(deposited)/$Si^{18}O_2$(thermally grown)/4H-SiC structure.[29] In fact, what is observed after PDA is a small shift in the opposite direction, towards higher proton energies, observed for all temperatures, as compared with the sample without PDA. This fact indicates N transport towards the substrate during annealing. Such an effect could be related to the electrical degradation observed. It is clear, from our results and from contrasting results reported in literature, that deeper investigation of PDAs in inert ambient must be performed to fully understand their consequences.

In summary, investigation of thermal nitridation of 4H-SiC in $^{15}NH_3$ was performed. In the temperature range investigated (900°C to 1100°C), significantly higher incorporation of nitrogen occurred in the Si substrate as compared with the SiC. For the SiC case, the nitrogen incorporation observed was in the form of nitrogen bonded only to silicon, or in the form of silicon oxynitrides. NRA investigation indicated that the presence of oxygen is due to, at least partially, its incorporation from air exposure. Electrical measurements of MOS capacitors with nitrogen confined to the SiO_2/4H-SiC interfacial region evidence high leakage currents and poor dielectric strength of the dielectric films. The quality of the dielectric films became even worse when PDA in Ar was performed, which induced transport of part of the N atoms towards the SiC substrate. Results suggest that modifications to the proposed route must be performed, aiming at nitrogen confinement to the SiO_2/4H-SiC interface and avoiding degradation of the dielectric film.

ACKNOWLEDGEMENTS

The authors would like to thank INCTs Namitec and Ines, MCT/CNPq, CAPES, and FAPERGS for financial support.

REFERENCES

1. J.B. Casady and R.W. Johnson, *Solid State Electron.* 39, 1409 (1996).
2. V. Presser and K.G. Nickel, *Crit. Rev. Sol. State* 33, 1 (2008).
3. S. Dhar, S. Wang, J.R. Williams, S.T. Pantelides, and L.C. Feldman, *MRS Bull.* 30, 288 (2005).
4. J. Rozen, A.C. Ahyi, X. Zhu, J.R. Williams, and L.C. Feldman, *IEEE Trans. Electron Devices* 58, 3808 (2011).
5. K. McDonald, M.B. Huang, R.A. Weller, L.C. Feldman, J.R. Williams, F.C. Stedile, I.J.R. Baumvol, and C. Radtke, *Appl. Phys. Lett.* 76, 568 (2000).
6. Y. Xu, X. Zhu, H.D. Lee, C. Xu, S.M. Shubeita, A.C. Ahyi, Y. Sharma, J.R. Williams, W. Lu, S. Ceesay, B.R. Tuttle, A. Wan, S.T. Pantelides, T. Gustafsson, E.L. Garfunkel, and L.C. Feldman, *J. Appl. Phys.* 115, 033502 (2014).
7. S.A. Corrêa, C. Radtke, G.V. Soares, L. Miotti, I.J.R. Baumvol, S. Dimitrijev, J. Han, L. Hold, F. Kong, and F.C. Stedile, *Appl. Phys. Lett.* 94, 251909 (2009).
8. J.A. Taillon, J.H. Yang, C.A. Ahyi, J. Rozen, J.R. Williams, L.C. Feldman, T.S. Zheleva, A.J. Lelis, and L.G. Salamanca-Riba, *J. Appl. Phys.* 113, 044517 (2013).
9. G. Liu, A.C. Ahyi, X. Yi, T. Isaacs-Smith, Y.K. Sharma, J.R. Williams, L.C. Feldman, and S. Dhar, *IEEE Electron Devices Lett.* 34, 181 (2013).
10. P. Fiorenza, F. Giannazzo, M. Vivona, A. La Magna, and F. Roccaforte, *Appl. Phys. Lett.* 103, 153508 (2013).
11. J.M. Fraser and F. Daniels, *J. Phys. Chem.* 62, 215 (1958).
12. R.J. Wu and X.T. Yeh, *Int. J. Chem. Kinet.* 28, 89 (1996).
13. K. McDonald, L.C. Feldman, R.A. Weller, G.Y. Chung, C.C. Tin, and J.R. Williams, *J. Appl. Phys.* 93, 2257 (2003).
14. X. Zhu, A.C. Ahyi, M. Li, Z. Chen, J. Rozen, L.C. Feldman, and J.R. Williams, *Solid State Electron.* 57, 76 (2011).
15. Q. Zhu, F. Qin, W. Li, and D. Wang, *Physica B* 432, 89 (2014).
16. A. Modic, Y.K. Sharma, Y. Xu, G. Liu, A.C. Ahyi, J.R. Williams, L.C. Feldman, and S. Dhar, *J. Electron. Mater.* 43, 857 (2014).
17. S. Wang, S. Dhar, S. Wang, A.C. Ahyi, A. Franceschetti, J.R. Williams, L.C. Feldman, and S.T. Pantelides, *Phys. Rev. Lett.* 98, 026101 (2007).
18. G. Chung, C.C. Tin, J.R. Williams, K. McDonald, M.D. Ventra, R.K. Chanana, S.T. Pantelides, L.C. Feldman, and R.A. Weller, *Appl. Phys. Lett.* 77, 3601 (2000).
19. G.Y. Chung, J.R. Williams, K. McDonald, and L.C. Feldman, *J. Phys. Condens. Matter* 16, S1871 (2004).
20. J. Rozen, M. Nagano, and H. Tsuchida, *J. Mater. Res.* 28, 28 (2013).
21. T. Yamakami, S. Suzuki, M. Henmi, Y. Murata, R. Hayashibe, and K. Kamimura, *Jpn. J. Appl. Phys.* 50, 01BG02 (2011).
22. H. Yang, D. Wang, and H. Nakashima, *J. Electrochem. Soc.* 159, H1 (2012).

23. W. Kern and D.S. Puotinem, *RCA Rev.* 31, 187 (1970).
24. I.J.R. Baumvol, *Surf. Sci. Rep.* 36, 1 (1999).
25. E. Pitthan, S.A. Corrêa, G.V. Soares, C. Radtke, and F.C. Stedile, *Nucl. Instrum. Methods Phys. Res. B.* 332, 56 (2014).
26. C. Driemeier, L. Miotti, R.P. Pezzi, K.P. Bastos, and I.J.R. Baumvol, *Nucl. Instrum. Methods Phys. Res. B* 249, 278 (2006).
27. T. Hosoi, T. Kirino, S. Mitani, Y. Nakano, T. Nakamura, T. Shimura, and H. Watanabe, *Curr. Appl. Phys.* 12, S79 (2012).
28. J.W. Chai, J.S. Pan, Z. Zhang, Q. Chen, and C.H.A. Huan, *Appl. Phys. Lett.* 92, 092119 (2008).
29. E. Pitthan, R. Palmieri, S.A. Corrêa, G.V. Soares, H.I. Boudinov, and F.C. Stedile, *ECS Solid State Lett.* 2, P8 (2013).
30. R. Kosugi, W. Cho, K. Fukuda, K. Arai, and S. Suzuki, *J. Appl. Phys.* 91, 1314 (2002).
31. S.K. Gupta, A. Azam, and J. Akhtar, *Semiconductors* 46, 545 (2012).
32. H. Li, S. Dimitrijev, D. Sweatman, H.B. Harrison, P. Tanner, and B. Feil, *J. Appl. Phys.* 86, 4316 (1999).
33. Z.Q. Zhong, Z.J. Sun, S.Y. Wang, L.P. Dai, and G.J. Zhang, *Eur. J. Appl. Phys.* 62, 20301 (2013).